

# Application of dispersion relations to $\eta\pi$ elastic scattering

Author: Johan Sebastián Guzmán Varela.

Facultat de Física, Universitat de Barcelona, Diagonal 645, 08028 Barcelona, Spain.\*

Advisor: Vincent Mathieu

**Abstract:** The existence of exotic mesons, particularly hybrid mesons, remains a subject of investigation. Among these, the meson  $\pi_1$  with  $J^{PC} = 1^{-+}$  is anticipated to be the lightest. In this study, we examine the reaction  $\eta^{(\prime)}\pi \rightarrow \eta^{(\prime)}\pi$  as  $\pi_1$  couples to the involved particles. By employing dispersion relations for various channels of this reaction, incorporating Regge forms, and conducting a partial wave expansion in both the forward and backward directions of the outgoing particles, we estimate the P-wave contribution associated with the purported  $\pi_1$  meson.

## I. INTRODUCTION

In the Standard Model of particle physics, gluons and quarks are the fundamental particles that carry color charge. Gluons mediate the strong interaction between quarks, which is governed by Quantum Chromodynamics (QCD).

The current quark model successfully describes the formation of quark systems such as mesons (composed of a quark and an antiquark) and baryons (composed of three quarks). However, it is postulated that more complex configurations are possible, such as hybrid mesons. Hybrid mesons consist of a quark-antiquark pair with an excited gluonic field that acts as a constituent, resulting in quantum numbers that are forbidden in the simple quark model. Lattice QCD computations, as demonstrated in [1], suggest that the  $\pi_1$  meson could be the lightest exotic hybrid meson, possessing the quantum numbers  $J^{PC} = 1^{-+}$ .

Therefore, one of the goals of the COMPASS experiment has been to study  $\eta^{(\prime)}\pi$  mesonic systems, as documented in [2]. These systems are expected to couple with the  $\pi_1$  hybrid meson. More recently, a new facility called GlueX has been developed as a complementary experiment to COMPASS, and its results are eagerly awaited and pending publication.

In this paper, a convenient scattering process is analyzed by studying its scattering amplitude  $A(s, t, u)$ . This allows for the establishment of a dispersion relation. An estimation for this relation may be given by using the Regge form, which is a valid approximation at high energies. The resulting identity is known as Finite Energy Sum Rule (FESR). Subsequently, a partial wave expansion is performed on the scattering amplitude to isolate the P-wave component, which is theorized to correspond to the  $\pi_1$  hybrid meson. Symmetries of the function  $A(s, t, u)$  in different channels of the  $\eta^{(\prime)} + \pi \rightarrow \eta^{(\prime)} + \pi$  reaction are utilized for this purpose. Finally, an expression is derived to estimate the integral over a range of energy of the P-wave of the amplitude using fitting tech-

niques applied to data from [3].

The structure of the paper is organized as follows: In Section II, the Mandelstam variables are introduced in Subsection II A, followed by an analysis of the channels and exchanged mesons in Subsection II B, and the establishment of dispersion relations and FESR using Regge forms in Subsection II D. Subsection II E then applies a series of approximations to derive an expression for estimation. Section III utilizes this expression along with fitting on experimental data to estimate the P-wave. Finally, Section IV presents the conclusions.

## II. DISPERSION RELATION

### A. Kinematics

The first step is to establish a framework of tools for effectively investigating a scattering reaction  $2 \rightarrow 2$ . Such reactions involve two Lorentz invariant variables, and a particularly advantageous set of variables known as the Mandelstam variables,  $s$ ,  $t$ , and  $u$ , prove to be valuable in this context.

Let  $\mathbf{p}_i$ , and  $\mathbf{p}'_i$  be the four-vectors of the incoming, and outgoing mesons  $i$ , for  $i = \pi, \eta$ . Then, the Mandelstam variables are defined as it follows:

$$\begin{aligned} s &\equiv (\mathbf{p}_\pi + \mathbf{p}_\eta)^2 & t &\equiv (\mathbf{p}_\pi - \mathbf{p}'_\pi)^2 & u &\equiv (\mathbf{p}_\pi - \mathbf{p}'_\eta)^2 \\ &= (\mathbf{p}'_\pi + \mathbf{p}'_\eta)^2 & &= (\mathbf{p}_\eta - \mathbf{p}'_\eta)^2 & &= (\mathbf{p}_\eta - \mathbf{p}'_\pi)^2, \end{aligned} \quad (1)$$

which implies that  $s+t+u = 2(m_\pi^2 + m_\eta^2) := \Sigma$ , and therefore only two Mandelstam variables are independent.

In the center-of-momentum (CM) frame, the conservation of energy and momentum ensures that the momenta satisfy  $p = |\vec{p}_1| = |\vec{p}_2|$ , and  $p' = |\vec{p}'_1| = |\vec{p}'_2|$ , and this relationship holds:

$$z_s = \cos \theta = 1 + \frac{t}{2p^2} = -1 - \frac{u - u_0}{2p^2}, \quad u_0 = \frac{(m_1 - m_2)^2}{s}. \quad (2)$$

\*Electronic address: j.guzmava28@alumnes.ub.edu

### B. Reaction $\pi + \eta \rightarrow \pi + \eta$

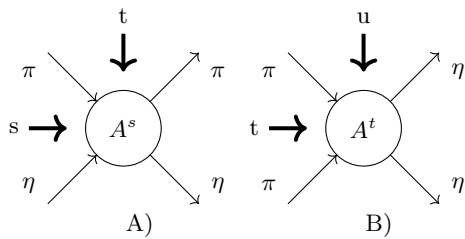


FIG. 1: Diagrams of the  $s$ - and  $t$ -channels for the  $\pi + \eta \rightarrow \pi + \eta$  reaction.

Fig. 1 A) portrays the reaction  $\pi + \eta \rightarrow \pi + \eta$ , and the order in which the mesons are arranged in the figure is labeled as the “ $s$ -channel”. When it is rotated by  $90^\circ$ , it resembles diagram B), except with a reversed direction for the  $\pi$  and  $\eta$  particles. This reversal is equivalent to exchanging the particles with their respective antiparticles. However, no differentiation will be needed between particles and antiparticles, and they will be treated interchangeably. Consequently, the resulting reaction is referred to as the  $t$ -channel, as  $t = (\mathbf{p}_\pi - \mathbf{p}_\pi)^2 = (\mathbf{p}_\pi + \bar{\mathbf{p}}_\pi)^2$  represents the energy associated with the collision between the particle and antiparticle, where  $\bar{\mathbf{p}}$  is the antiparticle’s four-vector. Similarly, the  $u$ -channel can be obtained analogously and is found to be equivalent to the  $s$ -channel.

In conclusion, each channel involves a specific pair of incoming and outgoing particles. These reactions occur through the mediation of an intermediate meson, which couples to both the incoming and outgoing pairs. In order for this reaction to take place, the coupling of the quantum numbers  $G$ , and  $I$  of the incoming, and outgoing particles (shown in Fig. 2) should coincide with that of the intermediate meson, whose quantum numbers are collected in Table I.

TABLE I: Naming scheme of mesons with their quantum numbers.

	$G=1$		$G=-1$	
	PC	Name	PC	Name
$I=0$	++	$f$	--	$\omega$
	-+	$\eta$	+-	$h$
$I=1$	--	$\rho$	++	$a$
	+-	$b$	-+	$\pi$

On the one hand, the restrictions on the  $s$ -channel are:

1.  $\pi\pi$  coupling: since the  $\pi$  meson has isospin  $I = 1$ , the coupling has  $I = 0, 1$ , or  $2$ ; and its intrinsic parity is  $G = +1$  because it is the result of the coupling of two equal particles. Then, according to Table I, the candidates are  $f_2$ , and  $\rho$ ,
2.  $\eta\eta$  coupling: since  $\eta$  has an isospin is  $I = 0$ , the coupling of the isospin is  $I = 0$ ; and  $G = 1$ . The

only compatible particle with these quantum numbers is  $f_2$ .

An additional constraint is the minimum energy for the scattering process to take place. Since  $\sqrt{s}$  coincides with the energy of the particles, this constraint results in a threshold for  $s$ , corresponding to the squared total rest mass of the incoming particles:  $s > s_0 = (m_\pi + m_\eta)^2$ , where  $m_\eta = 135$  MeV, and  $m_\pi = 140$  MeV [3].

On the other hand, the  $t$ -channel reaction is solely constrained by the  $\pi\eta$  coupling. This coupling is characterized by the isospin values of  $\eta$  and  $\pi$ , which yield a total  $I = 1$  for the system. Additionally, the intrinsic parity of  $\eta$  is  $G = +1$ , while that of  $\pi$  is  $G = -1$ , resulting in  $G = -1$  for the coupling. Consequently, the intermediate mesons in this channel can be either  $a_2$  or  $\pi_1$ . Moreover, the threshold of  $s$  is  $s_0^2 = (m_\pi + m_\pi)^2 = 4m_\pi^2$ .

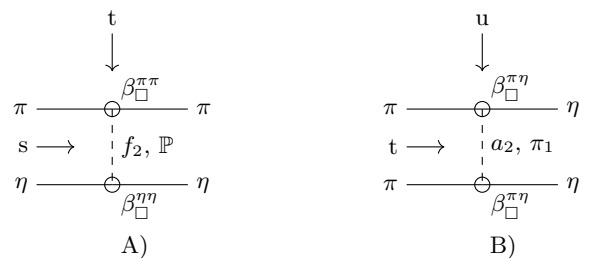


FIG. 2: Mesons exchanged during the reaction  $\pi + \eta \rightarrow \pi + \eta$  in different channels. A) shows the  $s$ -channel, and B) shows the  $t$ -channel.  $\beta_{\square}^{xy}$  is the coupling of the intermediate meson  $\square$  that couples to the particles  $x$ , and  $y$ .

### C. Change of variables: $\nu$ and $\nu'$

It is important to note that fixing either  $t$  or  $u$  in the equation  $s + t + u := \Sigma$ , along with the previously determined thresholds, results in the existence of prohibited points denoted as  $\{(s, u)\}$ , or  $\{(s, t)\}$ , respectively. These sets, known as cuts, introduce an asymmetry in the complex plane of  $\nu$  along the  $\text{Re}(\nu)$  axis with respect to 0.

Let the crossing variables  $\nu$ , and  $\nu'$  be defined as:

$$\nu = \frac{s - u}{2}, \quad \nu' = \frac{s - t + 4m_\pi^2 - (m_\pi + m_\eta)^2}{2}. \quad (3)$$

These variables allow to symmetrize the the two cuts at fixed  $t$ , and  $u$ , respectively:  $s(-\nu, t) = u(\nu, t)$ , and  $s(-\nu', u) = t(\nu', u)$ .

### D. Finite Energy Sum Rules (FESR)

In a stationary-state scattering process, the scattering amplitude  $A(s, t, u)$  quantifies the probability amplitude of an outgoing spherical wave with respect to the incoming plane wave. Due to the crossing symmetry arising

from CPT symmetry, this function describes all three channels  $s$ ,  $t$ ,  $u$  when evaluated in the corresponding domains, which exclude the respective thresholds mentioned in Section II C.

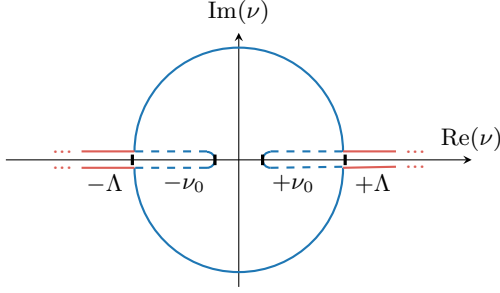


FIG. 3: Cauchy's integral theorem can be applied to the integral of the amplitude over the blue contour, and also over the solid one, allowing to identify the absolute values of the integrals over each distinct segment of the figure.  $\pm\nu_0$  limits of the cuts, and  $\Lambda > \nu_0$  is arbitrary.

The Regge form, given by  $A \propto \frac{1+\tau e^{-i\pi\alpha}}{-\sin \pi\alpha} \beta\nu^\alpha$ , where  $\alpha$  is the Regge trajectory, provides an approximation for the amplitude that holds true for large  $|\nu|$ ,  $|\nu| > \Lambda$  (Chapter 9 of [4]). Consequently, it is suitable for application over the orange segment illustrated in *Fig. 3*. In this context,  $\tau$  represents the signature factor, and due to the slow variation of  $\beta$ , it is reasonable to assume  $\beta(t) = \beta$ .

It is worth noting that the integrals of the amplitude over the segments that enclose the real axis in parallel correspond to the integral of the difference between the amplitude evaluated above and below the axis. This difference is proportional to  $\text{Im} A$  due to the Schwarz reflection principle. In conclusion, when considering the integrals over the orange segments in Figure 3, the integrand can be expressed as  $\text{Im} A = \tau\beta\nu^\alpha$ .

### 1. Fixed and small $t=x$

In this scenario, Eq. (2) indicates that  $\theta$  is a small angle. Consequently, the  $\pi$  meson is moving in the forward direction.

The value of  $\nu$ , and  $u_0$ , corresponding to the threshold value of  $s$ ,  $s_0 = (m_\eta + m_\pi)^2$ , and to  $t = x$ , can be expressed as  $\nu_0(x) = 2m_\pi m_\eta + \frac{x}{2}$ , and  $u_0$ , respectively. Due to the symmetry of  $\nu$  explained in Section II C, the integral over the blue and dashed line of Fig. 3 yields:

$$\begin{aligned} & \int_{s_0}^{s(\Lambda)} \text{Im} A(s, t, u) ds + \int_{u_0}^{u(\Lambda)} \text{Im} A(s, t, u) du = \\ & \left[ \int_{\nu_0(x)}^{\Lambda} \text{Im} A(s(\nu, t), t, u(\nu, t)) d\nu \right. \\ & \left. + \int_{-\nu_0(x)}^{-\Lambda} \text{Im} A(s(\nu, t), t, u(\nu, t)) d\nu \right] \left| \det(\mathbf{J}_f) \right|, \end{aligned} \quad (4)$$

where the absolute value of the Jacobian determinant is  $|\det(\mathbf{J}_f)| = 1$ .

This integral, as noted in the caption of Fig. 3, equals the integral over the orange segment of the figure. If this identity is then multiplied by  $\nu^k$ , with  $k \in \mathbb{N}$  so that the analytic behaviour of the integrand is not affected, and the change of variable  $\nu \rightarrow -\nu$  is applied to the last integral of Eq. (4), it yields:

$$\begin{aligned} & \int_{\nu_0(x)}^{\Lambda} \left[ \text{Im} A(s(\nu, t), t, u(\nu, t)) \nu^k \right. \\ & \left. + \text{Im} A(s(-\nu, t), t, u(-\nu, t)) (-\nu)^k \right] d\nu = \\ & \sum_{\pm} \int_{\pm\Lambda}^{\pm\infty} \beta \nu^{\alpha+k} d\nu = \sum_i [1 + \tau_i (-1)^k] \beta_i \frac{\Lambda^{\alpha_i+k+1}}{\alpha_i+k+1}. \end{aligned} \quad (5)$$

where the second integral has split into integrals in correspondence with the several particles  $i$  that mediate the process, and that were determined in Section II B.

The fact that the  $s$ - and  $u$ -channels are equivalent in this reaction, along with the symmetry of  $\nu$ , entails that  $A(s(-\nu, t), t, u(-\nu, t)) = A(u(\nu, t), t, s(\nu, t))$ .

Since this scenario corresponds to the  $t$ -channel,  $\tau = +1$ . Then,  $k$  must be even,  $k = 2n$ , because otherwise, Eq. (6) is trivial. The final expression is:

$$\begin{aligned} & \int_{\nu_0(x)}^{\Lambda} \text{Im} A(s(\nu, t), t, u(\nu, t)) d\nu = \\ & \left[ \beta_{\mathbb{P}}^{\pi\pi} \beta_{\mathbb{P}}^{\eta\eta} \frac{\Lambda^{\alpha_{\mathbb{P}}+2n+1}}{\alpha_{\mathbb{P}}+2n+1} + \beta_{f_2}^{\pi\pi} \beta_{f_2}^{\eta\eta} \frac{\Lambda^{\alpha_{f_2}+2n+1}}{\alpha_{f_2}+2n+1} \right]. \end{aligned} \quad (6)$$

### 2. Fixed and small $u=x$

In this scenario, Eq. (2) indicates that  $\theta$  represents a straight angle. Consequently, the  $\eta$  meson is moving in the forward direction, and  $\nu'_0(x) = (4m_\pi^2 - (m_\eta - m_\pi)^2 + x)/2$ .

Similarly to the case treated above, an expression similar to Eq. (5) may be retrieved if the crossing variable  $\nu'$  is used, instead of  $\nu$ :

$$\begin{aligned} & \int_{\nu'_0(x)}^{\Lambda'} \text{Im} \left[ A(s(\nu', u), t(\nu', u), u) \right. \\ & \left. + A(t(\nu', u), s(\nu', u), u) (-1)^k \right] \nu'^k d\nu' \\ & = \sum_i [1 + \tau_i (-1)^k] \beta_i(t) \frac{\Lambda^{\alpha_i+k+1}}{\alpha_i+k+1}. \end{aligned} \quad (7)$$

In this instance, however, there are two different possibilities for  $\tau$ :

1.  $\tau = -1$ , which implies that  $k$  is odd,  $k = 2n + 1$ :

$$\int_{\nu'_0(x)}^{\Lambda'} \text{Im} \left[ A(s(\nu', u), t(\nu', u), u) + A(t(\nu', u), s(\nu', u), u)(-1)^{2n+1} \right] \nu'^{2n+1} d\nu' = 2(\beta_{\pi_1}^{\pi\eta})^2 \frac{\Lambda'^{\alpha_{\pi_1} + 2n + 2}}{\alpha_{\pi_1} + 2n + 2}, \quad (8)$$

2.  $\tau = +1$  which implies that  $k$  is even,  $k = 2n$ :

$$\int_{\nu'_0(x)}^{\Lambda'} \text{Im} \left[ A(s(\nu', u), t(\nu', u), u) + A(t(\nu', u), s(\nu', u), u)(-1)^{2n} \right] \nu'^{2n} d\nu' = 2(\beta_{a_2}^{\pi\eta})^2 \frac{\Lambda'^{\alpha_{a_2} + 2n + 1}}{\alpha_{a_2} + 2n + 1}. \quad (9)$$

### E. Approximation

The main objective of this study is to estimate the integrals over the range of energies  $[\nu_0, \Lambda]$  of the P-wave of  $A(s, t, u)$ . To accomplish this, certain approximations and simplifications are employed.

Firstly, the exchange of a  $\pi_1$  meson in the  $t$ -channel, as depicted in Fig. 2 B), is exotic, implying that  $\beta_{\pi_1}^{\pi\eta}(u) \approx 0$  (and also  $\alpha_{\pi}(u) \ll 0$ ). Consequently, Eq. (8) can be simplified as:

$$\int_{\nu'_0(x)}^{\Lambda'} \text{Im} \left[ A(s(\nu', u), t(\nu', u), u) + A(t(\nu', u), s(\nu', u), u)(-1)^{2n+1} \right] \nu'^{2n+1} d\nu' = 0, \quad (10)$$

and since  $\Lambda'$  is arbitrary, it follows that  $\text{Im} A(s(\nu', u), t(\nu', u), u) = \text{Im} A(t(\nu', u), s(\nu', u), u)$ .

The next step involves performing a partial wave expansion on  $A(s, x, u)$ , and  $A(s, t, x)$  using the variables defined in Equation 2 and the Legendre polynomials,  $P_\ell(z)$ :

$$A(s, x, u) = 16\pi \sum_{\ell}^{\infty} (2\ell + 1) t_\ell(s) P_\ell(z_1), \quad z_1 = 1 + \frac{x}{2p_{\pi\eta}^2},$$

$$A(s, t, x) = 16\pi \sum_{\ell}^{\infty} (2\ell + 1) t_\ell(s) P_\ell(z_2), \quad z_2 = -1 - \frac{x - u_0}{2p_{\pi\eta}^2}. \quad (11)$$

Additionally, the Regge trajectories of  $a_2$  and  $f_2$  are equal,  $\alpha_{a_2} = \alpha_{f_2}$  [5]; and the approximation  $m_\pi \approx m_\eta$  is made, which implies that  $\nu_0(x) \approx \nu'_0(x)$ . In addition,  $\nu$ , and  $\nu'$  are dummy variables, and  $\Lambda = \Lambda'$  is fixed. With these considerations in mind, the Eqs. (6) and (9) may

be subtracted, resulting in the following equation for the P-wave ( $\ell = 1$ ):

$$48\pi \int_{\nu_0(x)}^{\Lambda} \text{Im} \left[ t_1(s(\nu, x) [P_1(z_1) - P_1(z_2)] \nu^{2n} \right] d\nu = 2\beta_{\mathbb{P}}^{\pi\pi}(t) \beta_{\mathbb{P}}^{\eta\eta}(t) \frac{\Lambda^{\alpha_{\mathbb{P}} + 2n + 1}}{\alpha_{\mathbb{P}} + 2n + 1} + 2 \left[ \beta_{f_2}^{\pi\pi}(t) \beta_{f_2}^{\eta\eta}(x) - (\beta_{a_2}^{\pi\eta}(x))^2 \right] \frac{\Lambda^{\alpha_{f_2} + 2n + 1}}{\alpha_{f_2} + 2n + 1} - \sum_{\ell \in \text{even}} \int_{\nu_0(x)}^{\Lambda} \text{Im} t_\ell(s_\nu) \Delta_\ell(\nu, x) \nu^{2n} d\nu, \quad (12)$$

where  $\Delta_\ell(\nu, x) = 16\pi(2\ell + 1) [P_\ell(z_1) - P_\ell(z_2)]$  is assumed to be negligible, since the recurrence relation of  $P_\ell$  indicates that  $\Delta_\ell$  vanishes when  $m_\eta \rightarrow m_\pi$  for  $\ell$  even.

### III. ESTIMATION OF THE P-WAVE

In the last section, the integral of the P-wave over a range of energies  $[\nu_0, \Lambda]$  is expressed in terms of a set of couplings,  $\beta$ . The objective of this section is to retrieve their numerical value in order to obtain an estimation of the integral.

In general, the cross section of a scattering reaction is:

$$\sigma = \frac{(\hbar c)^2}{s} \beta \left( \frac{s}{\bar{s}} \right)^\alpha, \quad (13)$$

where  $\bar{s}$  is a normalization factor and may be taken to be  $\bar{s} = 1 \text{ GeV}$ . Furthermore, in natural units,  $\hbar c = 1$  (otherwise,  $(\hbar c)^2 = 0.389 \text{ GeV}^2 \text{ mbarn}$ ), and the cross section may be written as  $\sigma = \beta S^{\bar{\alpha}}$ , where  $S = s/\bar{s}$ , and  $\bar{\alpha} = \alpha - 1$ .

The total cross section of a reaction can be modeled as  $\sigma_{\text{TOT}} = X S^{\bar{\alpha}_{\mathbb{P}}} + Y X^{\bar{\alpha}_{\mathbb{R}}}$ , with  $\bar{\alpha}_{\mathbb{P}} = 0.0808$ , and  $\bar{\alpha}_{\mathbb{R}} = -0.4525$  [5], where X and Y are the terms associated with the Pomeron, and the Reggeons, respectively. It is noteworthy that Y can be further decomposed into a sum of terms, each corresponding to a specific Reggeon. Then, the experimental data for hadron collisions from various experiments found in [3] can be fitted, as shown in Fig. 4, and the resulting parameters are used to solve the following system:

$$\begin{cases} \sigma_{pp} = (\beta_{\mathbb{P}}^{pp})^2 S^{\bar{\alpha}_{\mathbb{P}}} + \left( (\beta_{f_2}^{pp})^2 - (\beta_{\rho}^{pp})^2 + (\beta_{a_2}^{pp})^2 - (\beta_{\omega}^{pp})^2 \right) S^{\bar{\alpha}_{\mathbb{R}}}, \\ \sigma_{p\bar{p}} = (\beta_{\mathbb{P}}^{pp})^2 S^{\bar{\alpha}_{\mathbb{P}}} + \left( (\beta_{f_2}^{pp})^2 + (\beta_{\rho}^{pp})^2 + (\beta_{a_2}^{pp})^2 + (\beta_{\omega}^{pp})^2 \right) S^{\bar{\alpha}_{\mathbb{R}}}, \\ \sigma_{pn} = (\beta_{\mathbb{P}}^{pp})^2 S^{\bar{\alpha}_{\mathbb{P}}} + \left( (\beta_{f_2}^{pp})^2 + (\beta_{\rho}^{pp})^2 - (\beta_{a_2}^{pp})^2 - (\beta_{\omega}^{pp})^2 \right) S^{\bar{\alpha}_{\mathbb{R}}}, \\ \sigma_{\bar{p}n} = (\beta_{\mathbb{P}}^{pp})^2 S^{\bar{\alpha}_{\mathbb{P}}} + \left( (\beta_{f_2}^{pp})^2 - (\beta_{\rho}^{pp})^2 - (\beta_{a_2}^{pp})^2 + (\beta_{\omega}^{pp})^2 \right) S^{\bar{\alpha}_{\mathbb{R}}}, \\ \sigma_{\pi^\pm p} = \beta_{\mathbb{P}}^{pp} \beta_{\mathbb{P}}^{\pi\pi} S^{\bar{\alpha}_{\mathbb{P}}} + \left( \beta_{f_2}^{pp} \beta_{f_2}^{\pi\pi} \mp \beta_{\rho}^{pp} \beta_{\rho}^{\pi\pi} \right) S^{\bar{\alpha}_{\mathbb{R}}}. \end{cases} \quad (14)$$

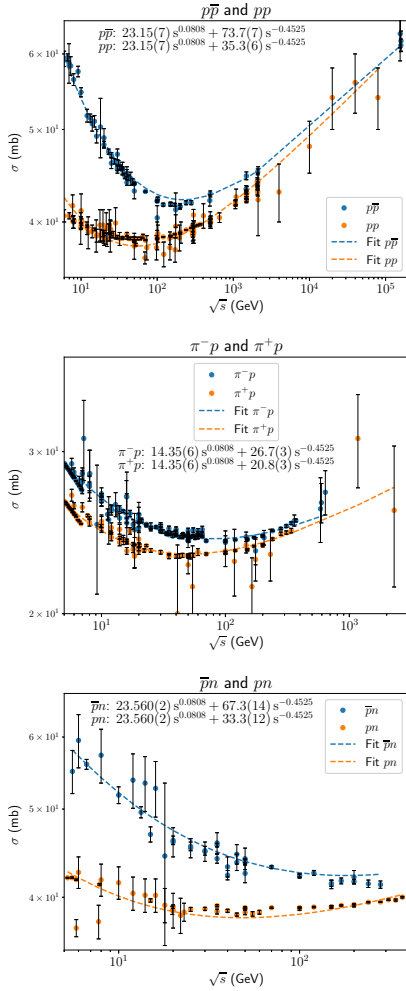


FIG. 4: Total cross section of the  $\bar{p}p$  and  $pp$ ;  $\pi^+p$  and  $\pi^-p$ ; and  $\bar{p}n$  and  $pn$  scattering processes, respectively, in function of the energy,  $\sqrt{s}$ .

The two relevant terms of the solution are presented:

$$\begin{aligned}\beta_{\mathbb{P}}^{\pi\pi} &= (2.982 \pm 0.013) \text{ mb}^{1/2}, \\ \beta_{f_2}^{\pi\pi} &= (3.28 \pm 0.06) \text{ mb}^{1/2}.\end{aligned}\quad (15)$$

The rest of the necessary couplings for the estimation of Eq. (12) can be retrieved via relations with the de-

cay widths of the channels of the reactions,  $\Gamma$ , and the momenta of the decay products,  $p$ , available at [3]:

$$\begin{aligned}\beta_{f_2}^{\eta\eta} &= \beta_{f_2}^{\pi\pi} \sqrt{\frac{\Gamma(f_2 \rightarrow \eta\eta)}{\Gamma(f_2 \rightarrow \pi^0\pi^0)}} \left(\frac{p_{\pi\pi}}{p_{\eta\eta}}\right)^{5/2} = (1.14 \pm 0.12) \text{ mb}^{1/2}, \\ \beta_{a_2}^{\pi\eta} &= \beta_{f_2}^{\pi\pi} \sqrt{\frac{\Gamma(a_2 \rightarrow \pi\eta)}{\Gamma(f_2 \rightarrow \pi^0\pi^0)}} \left(\frac{p_{\pi\pi}}{p_{\pi\eta}}\right)^{5/2} = (1.51 \pm 0.08) \text{ mb}^{1/2}.\end{aligned}\quad (16)$$

Similarly,  $\beta_{a_2}^{\pi\eta'} = (1.38 \pm 0.12) \text{ mb}^{1/2}$  by replacing  $\eta$  by  $\eta'$  (notice  $m_{\eta'} > m_{\pi}$  [3]). Also,  $\beta_{f_2}^{\eta'\eta'} = \beta_{f_2}^{\eta\eta} \tan^2 \theta_d = (0.96 \pm 0.10) \text{ mb}^{1/2}$  is found by using the  $\eta - \eta'$  mixing angle ( $\theta_d = 42.52^\circ$ ) found at [6]. Furthermore,  $\beta_{\mathbb{P}}^{\eta'\eta'} \approx \frac{120}{73} \beta_{\mathbb{P}}^{\eta\eta}$ , which is the quotient of the values corresponding to the channels  $\pi\eta$ , and  $\pi\eta'$  in Table 1 of [7].

TABLE II: Estimations of Eq. (12).  $\Lambda = 3 \text{ GeV}^2 \gg \nu_0$ .

	$n = 1$	$n = 2$	$n = 3$
$\eta$	$(95 \pm 3) \text{ mb GeV}$	$(427 \pm 13) \text{ mb GeV}^3$	$(2560 \pm 70) \text{ mb GeV}^5$
$\eta'$	$(147 \pm 4) \text{ mb GeV}$	$(668 \pm 14) \text{ mb GeV}^3$	$(4030 \pm 80) \text{ mb GeV}^5$

#### IV. CONCLUSION

In this study, we examined the scattering reaction  $\pi\eta^{(\prime)} \rightarrow \pi\eta^{(\prime)}$ , its channels, and it was argued that a single scattering amplitude function describes all of them.

We established dispersion relations for the different channels, in the forward and backward direction of the scattering. Then, Regge theory and a partial wave expansion were applied, yielding an expression for the integral of the P-wave amplitude, which corresponds to the  $\pi_1$  hybrid meson, within the low energy range of  $[\nu_0, \Lambda]$ .

We evaluated the integral using parameters derived from fitting experimental data. Interestingly, we found that the integrals were larger for  $\eta'$  than for  $\eta$ , which aligns with existing theoretical expectations.

Similarly, waves other than the P could have been studied, or a parametrization of the scattering amplitude could be used to estimate the integral in Eq. (12).

Throughout this work, the courses in Quantum Mechanics and Complex Analysis (Faculty of Mathematics) played a crucial role in achieving my objectives.

[1] C. A. Meyer and Y. Van Haarlem, Phys. Rev. C **82**, 025208 (2010).  
[2] C. Adolph et al., Physics Letters B **740**, 303 (2015).  
[3] Workman, R. L. et al. (Particle Data Group), Prog. Theor. Exp. Phys. **2022**, 083C01 (2022).  
[4] V. Gribov, *Strong Interactions of Hadrons at High Energies: Gribov Lectures on Theoretical Physics*, Cambridge Monographs on Particle Physics, Nuclear Physics and Cosmology (Cambridge University Press, 2023).

[5] A. Donnachie and P. Landshoff, Physics Letters B **296**, 227 (1992).  
[6] F. Ambrosino et al. (KLOE collaboration), Journal of High Energy Physics **2009**, 105 (2009).  
[7] L. Bibrzycki et al., The European Physical Journal C **81**, 647 (2021).